

Side-Chain Liquid-Crystal Polymers: Gel-like Behavior below Their Gelation Points

P. Martinoty,^{*,†} L. Hilliou,[†] M. Mauzac,[‡] L. Benguigui,^{†,§} and D. Collin[†]

Laboratoire de Dynamique des Fluides Complexes, Unité Mixte de Recherche U.L.P.- C.N.R.S. n° 7506, 4 rue Blaise Pascal, 67070 Strasbourg Cedex, France, and Laboratoire des Interactions Moléculaires et de Réactivité Chimique et Photochimique, Unité Mixte de Recherche U.P.S.-C.N.R.S. n° 5623, 118 route de Narbonne, 31062 Toulouse Cedex, France

Received August 17, 1998; Revised Manuscript Received December 30, 1998

ABSTRACT: We present microrheology experiments on a series of polysiloxane-type liquid-crystal polymers with mesogen-graft amounts of 25%, 70% and 100%. The experiments, conducted as a function of sample thickness, show that the low-frequency response of all of these polymers shifts progressively from a liquid-type behavior for thick samples ($>100\ \mu\text{m}$) to a purely elastic behavior for thin samples ($<20\ \mu\text{m}$). This surprising change in behavior, which occurs in all phases including the isotropic phase, points to the fact that these polymers do not behave like melts but like gels below their gelation point. Comparison of the results obtained in the nematic and isotropic phases shows that the clusters are not sensitive to the orientational order. The absence of any rubbery plateau (in the case of thick samples) and the simultaneous presence of a low-frequency elastic plateau (in the case of thin samples) are indicative of the existence of temporary knots of a new type, associated with interaction between the mesogens. We also present a confined-geometry percolation model and a model consisting of an association in parallel of the elastic and viscous regions which make up the sample. This latter model offers an explanation of the whole set of results obtained, unlike the percolation model in confined geometry.

1. Introduction

Side-chain liquid-crystal polymers are generally made up of polysiloxane- or polyacrylate-type chains onto the sides of which liquid-crystal molecules have been grafted by means of a flexible spacer. The presence of liquid-crystal molecules and a polymer chain generates competition between the tendency toward order imposed by the mesogenic elements and the tendency toward disorder imposed by the polymer chain. That is why these compounds have always been described as melts that are only differentiated from conventional melts by the appearance of a more or less pronounced anisotropy of the chains in their nematic and smectic phases.¹

The first proof that these melts do not comply with this image has been afforded by recent microrheology experiments carried out in the isotropic phase of a polysiloxane with a polymerization degree of $N=80$ and a polymethacrylate with $N=56$.² These experiments show that the low-frequency response of these materials shifts progressively from a liquid-type behavior for thick samples ($>100\ \mu\text{m}$), which is the behavior expected, to a purely elastic behavior for thin samples ($<20\ \mu\text{m}$). This surprising change in behavior has been explained by the presence of elastic clusters of macroscopic size, suggesting that these polymers do not behave like melts but like gels below their gelation point. These experiments have also shown the importance of anchoring conditions in the characterization of these compounds; strong anchoring to the surfaces of the sample-bearing slides on which the compound is placed allows the elastic behavior to show up, which is the real response of the compound, whereas weak anchoring leads to a

slip effect and, consequently, to an apparently liquid response. Strong anchoring is obtained for surfaces with grooves perpendicular to the shear.

In this article, we present measurements of the complex shear modulus in the isotropic (I), nematic (N) and smectic C (SmC) phases of a series of polysiloxanes with different mesogen amounts but having the same degree of polymerization. The purpose of these experiments, carried out as a function of the thickness of the samples studied, was to determine whether the clusters are sensitive to the mesomorphic phase considered and the amount of the grafted mesogens.

We also develop a confined-geometry percolation model and a model consisting of association in parallel of elastic and viscous regions; we demonstrate that it is this latter model alone which affords an explanation of the whole set of results obtained, suggesting that the structure of the clusters is different from that of the percolation clusters.

This paper is organized as follows: the materials and methods used are described in section II, the experimental results are reported in section III, the theory is presented in section IV, and the analysis and discussion of the results are given in section V.

II. Materials and Methods

The polymers studied correspond to the general formula which is given by Figure 1. They are obtained by substituting polysiloxane chains with various proportions y of mesogens. The precursor backbones are copolymers formed by hydrogenomethylsiloxane and dimethylsiloxane units. They are synthesized in such a way as to be of virtually identical lengths (degree of polymerization = 70 ± 5), and with a statistical distribution of the two types of units.³ The average molar weights were determined from absolute tonometrical measurements. The distribution of the weight is narrow, and the polydispersity index, as determined by steric exclusion chromatography, is on the order of 1.2. The amount and distribution of the two types of units were analyzed by ²⁹Si NMR.

[†] Laboratoire de Dynamique des Fluides Complexes.

[‡] Laboratoire des Interactions Moléculaires et de Réactivité Chimique et Photochimique.

[§] Permanent address: Solid State Institute, Technion, Israël Institute of Technology 32000 Haifa, Israël.

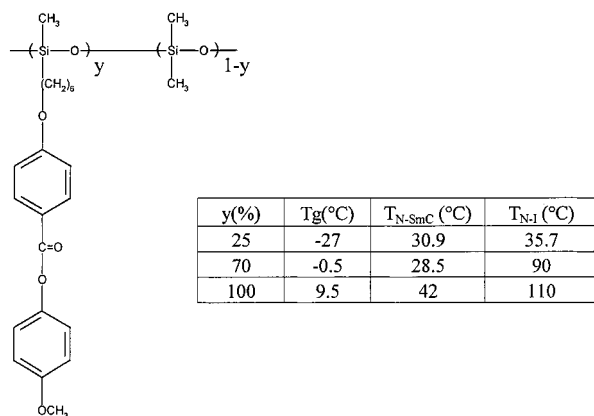


Figure 1. Molecular structure of the samples with their transition temperatures. $y(\%)$ is the mesogen-graft amount.

The mesomorphic polymers were prepared by a hydrosilylation reaction between the silane functions of the original backbones and the mesogenic groups bearing an end vinyl link.⁴ The reaction was performed at 60 °C in toluene solution, with dicyclopentadienyl-platinum chloride acting as a catalyst. For all of the polymers, the mesogenic groups were introduced in excess of 15% with regard to the silane function. The polymers were then purified by being precipitated twice in methanol. ¹H NMR analysis makes it possible to check that complete substitution of the silane functions has taken place.

The characteristics of the three mesomorphic polymers studied are given in Figure 1. The nature of the mesophases and the temperatures at which they occur were determined by polarized-light optical microscopy and differential scanning calorimetry (DSC). The transition temperatures recorded in Figure 1 correspond to those determined from the position of the DSC peaks (experimental error is less than ± 1 °C) as the temperature fell at 5 °C/min. The glass-transition temperatures (T_g) were obtained as the temperature increased at 10 °C/min.

Our experimental setup is an improved version of that developed by Cagnon and Durand⁵ some time ago. It operates on the principle of imposing a slight deformation on the sample, using a piezo-electric ceramic vibrating in shear mode, and then measuring the stress transmitted using a second ceramic. The strain imposed on the sample is given by

$$\epsilon = \frac{\delta}{L} \approx V_{\text{in}} = (V_0)_{\text{in}} e^{i\omega t} \quad (1)$$

where V_{in} is the tension applied to the emitting ceramic, δ is the resulting displacement, and L is the thickness of the sample. The stress measured on the receiving ceramic is given by

$$\sigma = \frac{f}{S} \approx V_{\text{out}} = (V_0)_{\text{out}} e^{i(\omega t + \varphi)} \quad (2)$$

where f is the force transmitted by the sample of surface area S , and V_{out} is the tension given out by the ceramic. Phase change φ can vary from zero (perfectly elastic solid) to $\pi/2$ (Newtonian liquid). Measurement of the complex shear modulus

$$G = \frac{\sigma}{\epsilon} \approx \frac{(V_0)_{\text{out}}}{(V_0)_{\text{in}}} e^{i\varphi} \quad (3)$$

enables the nature and mechanical properties of the compound to be determined.

In practice, the compound is placed between two glass slides, one of which is stuck to the emitting ceramic and the other to the receiving ceramic. Sample thickness ranged from 10 to 120 μm , and the surface area was ~ 2 cm^2 . For all thicknesses, deformation ϵ was on the order of 10^{-3} . The temperature of

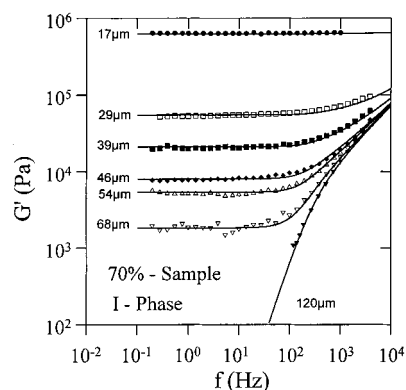


Figure 2. Real part, G' , of the shear modulus as a function of frequency in the isotropic phase of the 70% sample. The results obtained show that the low-frequency part of G' shifts progressively from a liquid-type behavior ($G' \approx \omega^2$) to an elastic type ($G' = \text{constant}$) as thickness decreases. The solid lines are the fits made with eq 6, on the basis of the existence of elastic clusters (see text).

the cell was regulated to within $\pm 10^{-2}$ °C, and the glass slides were adjusted for parallelism to within $\pm 10^{-4}$ rad. The cell was calibrated using solid or liquid materials with known compression and viscosity moduli, respectively.

To avoid any slip of the polymer on the glass slides on which the samples were placed, these latter had grooves made mechanically on their surfaces using diamond paste (with 0.25 μm diamond particles), perpendicular to the shear. It should, however, be noted that the value of the real part G' of the complex shear, measured at low frequency, may vary slightly from one cell to another. We think that this is due to the fact that the surfaces are not completely identical, even though they were all prepared in the same way.

Because G' is sensitive to the anchoring quality, comparison between measurements associated with different thicknesses or between those belonging to two different phases is only pertinent if the anchoring remains unchanged. This is why measurements as a function of thickness were taken while the interceramic distance was reduced but without ever opening the cell. Measurements were taken in the I and N phases of the 25%, 70%, and 100% samples and in the SmC phase of the 25% sample.

Each sample was introduced into the cell in the isotropic phase ($T = 110$ °C for the 70% sample; $T = 118$ °C for the 100% sample; $T = 44$ °C for the 25% sample), and a measurement was taken at this temperature. The sample was then cooled to a temperature chosen to be within its nematic state ($T = 75$ °C for the 100% sample; $T = 70$ °C for the 70% sample; $T = 34$ °C for the 25% sample). After a measurement was taken at this temperature, the sample was brought back into the isotropic phase at the starting temperature. The interceramic distance was then reduced, and a measurement was taken for this new thickness. The sample was then cooled to the temperature chosen previously within its nematic domain, and a new reading was taken. This method, followed for all sample thicknesses, makes it possible to compare the results obtained in the I and N phases. In the case of the SmC phase of the 25% sample, the sample was introduced into the cell in its nematic phase at $T = 35$ °C, and measurements were taken in the SmC phase at $T = 25$ °C.

III. Results

Typical examples showing the behavior of G' in the nematic and isotropic phases of the various polymers studied are given in Figures 2 (the 70% sample in its isotropic phase), 3 (100% sample in its nematic phase), and 4 (25% sample in its nematic phase). Figure 5 shows that the behavior observed in the smectic C phase of the 25% sample resembles those observed in the ne-

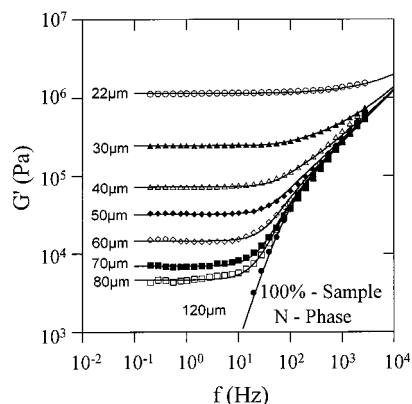


Figure 3. Same as for Figure 2 but for the nematic phase of the 100% sample.

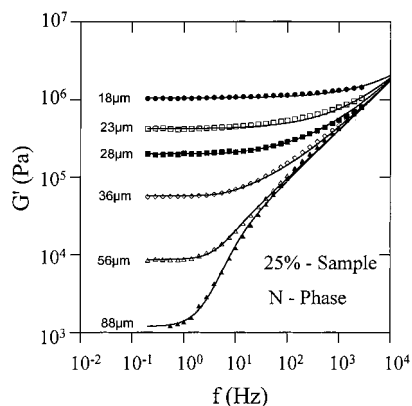


Figure 4. Same as for Figure 2 but for the nematic phase of the 25% sample.

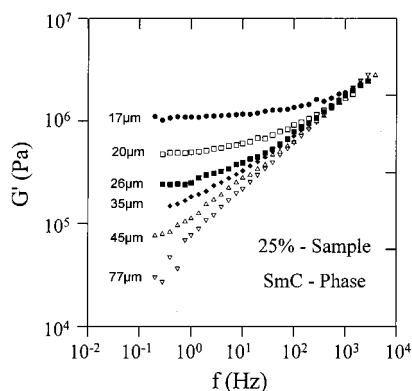


Figure 5. Same as for Figure 2 but for the smectic C phase of the 25% sample.

matic and isotropic phases but differs from them in that the elastic plateau shifts toward lower frequencies. The fact that the low-frequency response of G' shifts progressively from a liquid-type behavior to a solid-type as thickness decreases indicates that these polymers are constituted by elastic clusters made up of connected chains and separated from each other by free chains; in other words, these polymers behave like emergent gels. This hypothesis is upheld by the results given in Figure 6, which show that the behaviors of G' and G'' associated with the thick samples resemble those observed for a gel below its gelation point.⁶

We have also taken measurements at a given temperature as a function of time on samples 13 μm thick. The results obtained in the N and SmC phases of the

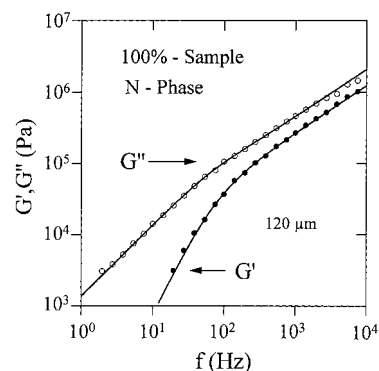


Figure 6. Real part, G' , and imaginary part, G'' , as a function of frequency for a thickness of $\sim 120 \mu\text{m}$ in the isotropic phase of the 100% sample. The solid lines are the fits made with eqs 6 and 7 (see text). The behavior of G' and G'' is similar to that observed for a gel below its gelation point.

Table 1. Parameters Obtained by Fitting Eqs 6 and 7 with G' and G'' Data (See Text)

sample	temperature ($^{\circ}\text{C}$)	x	$u = 1 - \beta$	$\eta (\text{Pa s}^{-1})$	τ (s)
25%	43.8 (isotropic)	4.2	0.64	195	7×10^{-3}
	33.8 (nematic)	4.3	0.64	695	2×10^{-2}
70%	110 (isotropic)	4.2	0.67	8	7×10^{-4}
	70 (nematic)	4.3	0.67	201	2×10^{-2}
100%	118 (isotropic)	4.4	0.66	8	1×10^{-4}
	75 (nematic)	4.3	0.66	221	3×10^{-3}

100% sample show that G' does not vary over a period of several days. On the other hand, the results obtained in the isotropic phase at $T = 140^{\circ}\text{C}$ show that G' decreases gradually over time (G' goes from a few 10^5 Pa to a few 10^4 Pa over a 12-h period).⁷ This decrease is less marked for lower temperatures and is hardly visible any longer at 112°C (i.e., 2°C above the N–I transition temperature). The results obtained on the 25% sample show that G' does not vary over time for temperatures lower than 100°C . Because this compound only becomes nematic at temperatures below 40°C , this result indicates that it is the temperature rather than the nature of the mesomorphic phase which controls the behavior of G' over time. Because the relaxation times of the clusters are in the *ms* range (see Table 1), these observations suggest that anchoring quality decreases gradually over time for very high temperatures.

IV. Theory

Below, we shall present two models which are different in nature but which both predict a shift from a liquid-type behavior to an elastic-solid one as sample thickness decreases.

(1) Association in Parallel of an Elastic Solid and a Viscoelastic Liquid. This model assumes the existence of (i) elastic clusters large enough to touch both of the sample-bearing slides, on one hand, and on the other hand, (ii) viscous regions composed of free chains and clusters which are not large enough to touch both of the sample-bearing slides. The distribution of relaxation times which reflects the relaxation times of the various clusters is described by a Cole–Davidson-type law, which respects the asymptotic behaviors observed for the thick samples ($G' \approx \omega^2$ and $G'' \approx \omega$ at low frequency; $G' \approx G'' \approx \omega^u$ at high frequency).

In the case of an association in parallel of elastic and viscous regions, the stress transmitted by these two regions are written respectively as:

$$\sigma_e = \chi G_S \frac{\delta}{L} \text{ and } \sigma_v = (1 - \chi) \frac{i\omega\eta}{(1 + i\omega\tau)^\beta} \frac{\delta}{L} \quad (4)$$

where L represents sample-thickness, δ is the movement imposed by the emitting ceramic, G_S is the rigidity modulus of the elastic regions, η is the viscosity of the polymer, and τ is the relaxation time of the largest cluster. β is the exponent associated with the Cole-Davidson law. β ranges from 0 (infinite relaxation time) to 1 (single relaxation time). The proportion of clusters which touch both sample-bearing slides is given by the ratio $\chi = s/S$, where S is the total area of the sample and s is the area of the elastic regions in simultaneous contact with both slides. We assume that χ varies with thickness according to the following law:

$$\chi = \left(\frac{L}{L_0}\right)^{-x} \quad (5)$$

where L_0 is the distance for which sample response is completely elastic. Equation 5 is valid for $L \geq L_0$.

Equation 4 makes it possible to deduce the real and imaginary parts of the complex shear modulus, which are given by

$$G'_{\text{app}} = G_S \chi + (1 - \chi) \omega \eta \sin \beta \theta / (1 + \omega^2 \tau^2)^{\beta/2} \quad (6)$$

$$G''_{\text{app}} = (1 - \chi) \omega \eta \cos \beta \theta / (1 + \omega^2 \tau^2)^{\beta/2} \quad (7)$$

where

$$\theta = \arctan(\omega\tau) \quad (8)$$

This model, used earlier,² assumes that all of the clusters have the same rigidity modulus, called G_S , and that viscosity η and time τ are independent of sample thickness. Variation of G with thickness comes from parameter χ alone.

(2) Percolation in Confined Geometry. The percolation theory has been used to describe the sol-gel transition.⁸ We shall apply this theory to our systems, as they have a behavior which relates them to gels below their percolation threshold.

The sol-gel transition is characterized by both a divergence of viscosity η as the gel-point (identified with the percolation threshold) is approached and the emergence of an elastic modulus G above this point. G and η obey the following power-law behavior:

$$\text{for } p < p_c \quad \eta = \eta_0 |p - p_c|^{-S} \quad (9)$$

$$\text{for } p > p_c \quad G = G_0 |p - p_c|^T \quad (10)$$

where η_0 and G_0 are linked to the microscopic properties of the medium. p represents the degree of connectivity, and p_c is the value of p at which the size of the largest cluster tends to infinity.

These results concern infinite samples, or more precisely samples whose size L is larger than their correlation length ξ . This quantity diverges in the vicinity of p_c , both above and below the threshold, with the power-law

$$\xi = L_0 |p - p_c|^{-\nu} \quad (11)$$

Below p_c , this characteristic length can be associated with the largest clusters, but above p_c , it concerns the largest clusters which are different from the infinite cluster.

For situations for which $L \leq \xi$, the concept of finite-size scaling has been proposed.⁹ This consists of expressing the various quantities as a function of $|p - p_c|$ and correlation length ξ . We have seen that above p_c , the elastic modulus increases in the same manner as $|p - p_c|^T$, but very near p_c , some finite clusters are of a size which is on the order of the sample size, and the effective modulus may be larger than its value for $L \rightarrow \infty$. In particular, at $p = p_c$ and for $p < p_c$, a nonzero G can be measured, because of the effect of finite size.

The principal results concerning the mechanical behavior of percolating systems are developed in the Appendix. We simply present below the more general case in which the asymptotic behavior of the elastic modulus G is a function of frequency and sample size.

For $\omega \rightarrow \infty$, and/or $p = p_c$

$$G \approx G' = G_0 \left(\frac{\omega}{\omega_0}\right)^{T(T+S)} \quad (12)$$

and for $\omega \rightarrow 0$,

$$G = G_0 \left[m_{\pm}(p) \left(\frac{L}{L_0}\right)^{-T\nu} + \left(\frac{\omega}{\omega_0}\right)^2 \left(\frac{L}{L_0}\right)^{(2S+T)\nu} + i \left(\frac{\omega}{\omega_0}\right) \left(\frac{L}{L_0}\right)^{S\nu} \right] \quad (13)$$

Equations 12 and 13 are eqs A12 and A14 of the Appendix. The function $m_{\pm}(p)$ is equal to one, and $m_{\pm}(p)$ is a function which is unknown. Sign + is for $p > p_c$, and sign - is for $p < p_c$. S and T are exponents associated with the viscosity and the elastic modulus, respectively (see eqs 9 and 10). The variables ν and L_0 are defined by the correlation length (see eq 11). G_0 is linked to the microscopic properties of the medium (see eq 10), and ω_0 is linked to the relaxation time of the largest cluster (see eq 15c below).

Equation 13 must be identical to that given by association in parallel of a perfect elastic solid and a viscoelastic liquid.

$$G = G_{\text{sol}} + \omega^2 \eta \tau + i \omega \eta \quad (14)$$

which means that we can write

$$\eta = \frac{G_0}{\omega_0} \left(\frac{L}{L_0}\right)^{S\nu} \quad (15a)$$

$$G_{\text{sol}} = G_0 m_{\pm}(p) \left(\frac{L}{L_0}\right)^{-T\nu} \quad (15b)$$

$$\tau = \frac{1}{\omega_0} \left(\frac{L}{L_0}\right)^{(T+S)\nu} \quad (15c)$$

These formulas are only valid for low-thickness samples ($L \rightarrow 0$), whereas eqs 6 and 7, which relate to the previous model, are valid whatever the thickness ($0 \leq \chi \leq 1$). This difference stems essentially from the fact that, in the previous model, the clusters have the same shear modulus G_S whatever their size, unlike the confined-geometry percolation model, which predicts a different shear modulus for each cluster. It should also be pointed out that length L_0 does not have the same

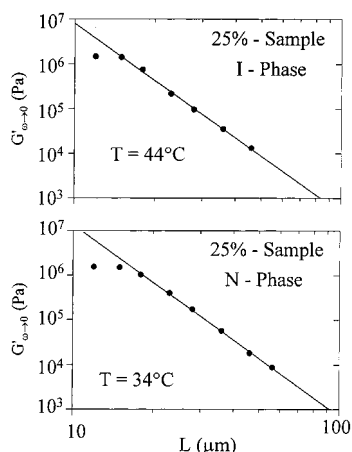


Figure 7. Variation of the low-frequency elastic plateau G' as a function of thickness in the isotropic and nematic phases of the 25% sample. G' varies according to a power law and saturates for low thicknesses at a value of $\sim 10^6$ Pa.

significance for each of the models. In the case of association in parallel, L_0 represents the thickness for which the behavior of G is totally elastic (eq 5). In the percolation model, L_0 is related to the correlation length (eq 11) and is associated with the microscopic properties of the system. Finally, it should also be noted that the percolation model predicts that G' and G'' are independent of thickness in the high-frequency regime ($\omega > \tau^{-1}$), whereas they depend on the latter in the case of association in parallel.

IV. Analysis of the Results and Discussion

We shall begin by considering the results obtained for G' and analyzing the variation of the low-frequency elastic plateau with thickness. Figure 7 corresponding to the 25% sample gives a typical example of the behaviors observed in the nematic and isotropic phases of the various polymers studied. It shows that the value of the elastic plateau increases as thickness decreases according to a power law, and then saturates for thicknesses of order of $15 \mu\text{m}$. Exponent x of the power law is the same for both phases, within the limits of experimental error ($x = 4.3$ in the nematic phase, and $x = 4.2$ in the isotropic phase). This result indicates that the clusters are not sensitive to the orientational order.¹⁰ It should also be noted that the data obtained for the thick samples ($120 \mu\text{m}$) in their I and N phases superimpose by a shift along the frequency axis. This overlap shows that the empirical principle of time-temperature superimposition operates across the transition, as has already been observed elsewhere.¹¹ This highlights again that the orientational order plays a minor role in the rheological properties of these polymers. Exponent x does not vary significantly for the samples with mesogen amounts of 70% and 100% as can be seen in Figure 8 relative to the 100% sample. This figure also shows that the low-frequency elastic plateau appears for a thickness which is higher in the N phase than in the I phase. This indicates that the size of the clusters decreases as the temperature increases. The same observation can be made in Figure 7. However, the effect is less visible in this case because the measurements were made at temperatures closer than those considered in Figure 8. It should be noted that x cannot be determined in the smectic C phase of the 25% sample, because of the shift of the elastic plateau toward

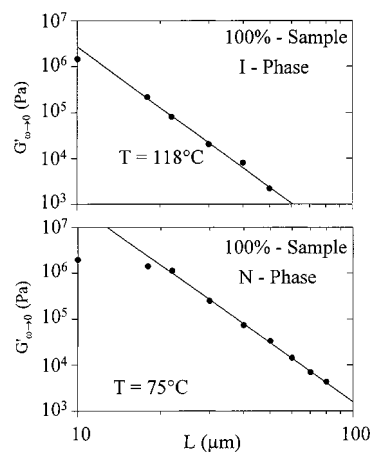


Figure 8. Same as for Figure 7 but for the 100% sample.

frequencies lower than those used in the experiment (cf. Figure 5). The analyses given below will therefore only refer to the results obtained in the nematic and isotropic phases of the various samples.

We shall first consider the results obtained for the thick samples ($L \sim 120 \mu\text{m}$), for which G' does not have low-frequency elastic behavior. These results were analyzed with eqs 6 and 7. Two different analyses were carried out: in one of them, we imposed the value of the elastic plateau deduced from the power laws determined above (for the 70% sample, for instance, this plateau has a value of ~ 200 Pa for a thickness of $120 \mu\text{m}$). In the other, this plateau was assumed to be zero ($\chi = 0$). Both analyses give identical results; the nonzero value of the plateau being too low, within the frequency domain studied, to alter the behavior of G' as ω^2 . An example which shows the good agreement of the solid-line fit and the experimental plot is offered by Figure 6. The values of the adjustable parameters (η , τ , β) obtained for the three samples are given in Table 1.

We shall now determine whether the behavior observed at high thicknesses is compatible with that observed at low thicknesses. To do this, we *simultaneously* analyzed all of the data giving the behavior of G' and G'' as a function of thickness and frequency. This analysis was conducted using eqs 6 and 7 with parameters η , τ , β , and x fixed at their previously determined values. For each thickness, we also imposed the measured value of the elastic plateau. The only adjustable parameter is therefore the length L_0 associated with the definition of χ (eq 5).

The fits made are shown as solid lines in Figures 2–4 (behavior of G') and in Figure 9, which gives an example of the behavior observed for G'' (100% sample). For reasons of clarity, only the data and the fits associated with 22, 30, and $120 \mu\text{m}$ are shown in Figure 9. The departure between these fits and the measurements of G'' taken at frequencies above 10^3 Hz is due to the influence of the glass transition. This influence also exists on the measurements of G' , albeit less visibly.

The very good agreement between the fits and the experimental plots associated with frequencies below 10^3 Hz indicates that the behaviors observed for both high and low thicknesses are of the same origin, i.e., the clusters. Terminal time τ is therefore not a polymer time but, rather, the time of the largest cluster. Length L_0 is on the order of $15 \mu\text{m}$ for all of the samples and is in good agreement with those directly deduced from the

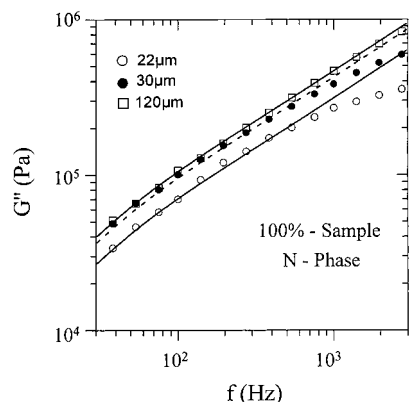


Figure 9. Variation of the imaginary part, G'' , of the complex shear modulus in the isotropic phase of the 100% sample, showing that G'' diminishes as thickness decreases. The solid line is the fit made with eq 7. The departure from the fit which appears for frequencies above 10^3 Hz is due to the influence of the glass transition (see text).

saturation of the low-frequency plateau of G' . This shows the complete consistency of the model.

Within the framework of the confined-geometry percolation model, exponent x is T/ν (see eq 15). However, the value of x determined experimentally ($x \sim 4$) is much higher than the values of T/ν expected for the 3D percolation models (T/ν is 2.1 for the electrical analogy and 3 for the Rouse model).⁶ The percolation model also predicts that G' and G'' must be independent of L in the high-frequency regime. However, the results obtained show that G' and G'' vary with thickness, as can be seen, for example, in Figure 9. These two observations show that the confined-geometry percolation model does not apply.

Two fundamental questions can be asked. What is the interaction between the chains which is at the origin of the clusters formation? Why does the system make macroscopic clusters rather than a network of infinite size?

We suggest two possible mechanisms which would allow the chains to be linked to each other. One of them is specific to side-chain liquid-crystal polymers. It has been considered earlier² and assumes the formation of clusters to be due to nematic interaction between the mesogens, forcing them to take up parallel alignment. The other mechanism assumes the formation of clusters to stem from transient friction between the chains, increased by the presence of the mesogens. This mechanism is a more general one and should apply to comb polymers with nonliquid-crystal side chains. Measurements taken on polymers obtained by replacing the mesogens with flexible aliphatic chains should make it possible to decide between these two possibilities. It should be noted that the clusters may possibly be related to the concept of random-orientational order recently introduced for nematic elastomers, which involves a macroscopic length associated with the disorder produced by the network acting as a random field.¹²

The finite size of the clusters is more difficult to explain, but it is probably due to the nature of the cross-links. In the case of conventional polymers, entanglements of the chains act as cross-links, and G' has an elastic response at finite frequency, which constitutes the rubbery plateau. In that regime, the polymer behaves like a dynamic network of infinite size. In the present case, the cross-links are different in nature, G' having no rubbery plateau; the polymer remains in a

pre-gel regime, and the elastic response can only be observed by varying the size of the sample.

The influence of molecular weight on cluster formation is also an important question. Experiments on thick samples by Kannan et al.¹³ show that the rheological behavior of high-molecular-weight polymers ($M_w \approx 10^6$ g/mol) is completely different from that of low-molecular-weight polymers ($M_w \leq 10^5$ g/mol). This change in behavior is characterized by a decrease in the shear modulus at T_{NI} , the appearance of a rubbery plateau, and orientational effects under flow. It would therefore be interesting to find out whether the size effects observed for low-molecular-weight polymers are modified (or even suppressed) for high-molecular-weight polymers.

V. Conclusion

In this article, we have studied a series of side-chain polysiloxanes with mesogen-graft amounts of 25%, 70% and 100%, with the other parameters being identical. We have shown that these polymers behave like gels below their gelation point, because of the presence of elastic clusters which are macroscopic in size and which occur in all phases, including the isotropic phase. Formation of these clusters does not depend on the mesogen-graft amounts. Experiments on samples with amounts lower than 25% would make it possible to determine the critical amount (should it exist) below which the clusters disappear. Comparison of the results obtained in the I and N phases shows that the clusters are not sensitive to the orientational order.

The absence of any rubbery plateau (observed for thick samples), which is a result of the low molecular weight of the polymer, and the simultaneous presence of a low-frequency elastic plateau (observed in the case of thin samples) are indicative of the existence of temporary knots of a new type. These knots are very probably associated with interaction between the teeth of the comb which, by slowing down diffusion of the chains very considerably, leads to the formation of clusters, as in the case of a physical gel, below the gelation point.

Although these systems behave like emergent gels, the percolation theory and its extension to confined geometry cannot explain the whole set of results. They can, however, be explained quantitatively by association in parallel of elastic and viscous regions, the latter being made up of clusters which all have the same rigidity modulus. The fundamental question which is now posed is why these systems make clusters rather than a network of infinite size. Another important question is whether these clusters are specific to side-chains liquid-crystal polymers or whether they also exist in other polymeric systems.

Note Added in Proof

We have recently shown that a side-chain polysiloxane, in which the mesogens have been replaced by flexible aliphatic chains with 15 carbons, presents a rheological behavior which is qualitatively similar to that observed in side-chain liquid-crystal polymers. This result shows that the clusters are not specific to these latter compounds and answers one of the questions raised in this article. We would like to thank J. J. Zanna for synthesizing the compound for us.

Acknowledgment. Partial support by the Ministère des Affaires Étrangères through PROCOPE project

96096 and Arc-en-ciel 98 Project 21 is gratefully acknowledged. L.B. thanks D. Stauffer for useful discussion on percolation in confined geometry.

APPENDIX

Shear Modulus near the Percolation Threshold as a Function of the Sample Size and the Frequency. (a) The Shear Modulus as a Function of Sample Size. The finite-size scaling theory⁹ establishes that G is given by

$$G \approx |p - p_c|^T f_{\pm} \left(\frac{L}{L_0} |p - p_c|^\nu \right) \quad (\text{A1})$$

(+ for $p > p_c$ and - for $p \leq p_c$).

The precise form of the scaling function f_{\pm} is to be determined, but its asymptotic behaviors are known because eq 10 must be recovered when $L \rightarrow \infty$, and G must be independent of $p - p_c$ when $L \rightarrow 0$; this last condition leads to $G \approx L^{-T\nu}$.

(b) The Elastic Modulus as a Function of Frequency. For large samples, G is expected to follow the following law⁶

$$G = G_0 |p - p_c|^T g_{\pm} \left(i \frac{\omega}{\omega_0 |p - p_c|^{T+S}} \right) \quad (\text{A2})$$

The frequency $\omega^* = \omega_0 |p - p_c|^{T+S}$ corresponds to the inverse of the relaxation time of the largest cluster, and g_{\pm} is a scaling function.

As in part a, the asymptotic behaviors of G can be deduced from those of g_{\pm} and are given by

for $\omega \rightarrow 0$ and $p < p_c$

$$G(\omega) = G_0 \left(\frac{\omega}{\omega_0} \right)^2 |p - p_c|^{-(2S+T)} \quad (\text{A3})$$

$$G'(\omega) = G_0 \left(\frac{\omega}{\omega_0} \right) |p - p_c|^{-S} \quad (\text{A4})$$

for $\omega \rightarrow 0$ and $p > p_c$

$$G(\omega) = G_0 |p - p_c|^T + G_0 \left(\frac{\omega}{\omega_0} \right)^2 |p - p_c|^{-(2S+T)} \quad (\text{A5})$$

$$G'(\omega) = G_0 \left(\frac{\omega}{\omega_0} \right) |p - p_c|^{-S} \quad (\text{A6})$$

for $\omega \rightarrow \infty$ whatever the value of p , or for $p = p_c$

$$G = G' = G_0 \left(\frac{\omega}{\omega_0} \right)^{T(T+S)} \quad (\text{A7})$$

(c) The Elastic Modulus as a Function of Frequency and Sample Size. For the more general case in which sample size L can be larger or smaller than the correlation length, we propose the following expression:

$$G = G_0 |p - p_c|^T h_{\pm} \left[\left(\frac{L}{L_0} \right) |p - p_c|^{-\nu}, i \frac{\omega}{\omega_0 |p - p_c|^{T+S}} \right] \quad (\text{A8})$$

which allows to recover the two preceding cases by making

$$h_{\pm}(x, 0) = f_{\pm}(x) \text{ for } \omega \rightarrow 0 \quad (\text{A9})$$

$$h_{\pm}(\infty, iy) = g_{\pm}(iy) \text{ for } L \rightarrow \infty \quad (\text{A10})$$

For $\omega \rightarrow \infty$ or $p \rightarrow p_c$ or both, $h_{\pm}(x, iy \rightarrow \infty)$ is expected to follow

$$h_{\pm}(x, iy \rightarrow \infty) \approx (iy)^{T(T+S)} \quad (\text{A11})$$

which leads to

$$G = G' = G_0 \left(\frac{\omega}{\omega_0} \right)^{T(T+S)} \quad (\text{A12})$$

For $L \rightarrow 0$, we propose that $h_{\pm}(x, y)$ be written

$$h_{\pm}(x, y) = m_{\pm}(p) x^{-T\nu} + iy x^{S\nu} + y^2 x^{(2S+T)\nu} \quad (\text{A13})$$

where $m_{+}(p)$ is equal to one, and $m_{-}(p)$ is unknown. The choice of the exponents of x is imposed by the fact that G must be independent of $|p - p_c|$ and only depends on L . Thus, $G(L, \omega)$ is written

$$G = G_0 \left[m_{\pm}(p) \left(\frac{L}{L_0} \right)^{-T\nu} + \left(\frac{\omega}{\omega_0} \right)^2 \left(\frac{L}{L_0} \right)^{(2S+T)\nu} + i \left(\frac{\omega}{\omega_0} \right) \left(\frac{L}{L_0} \right)^{S\nu} \right] \quad (\text{A14})$$

References and Notes

- (1) For instance, see: *Side-chain Liquid Crystal Polymers*, McArdle, C. B., Ed.; Blackie: Glasgow, 1989.
- (2) Gallani, J. L.; Hilliou, L.; Keller, P.; Martinoty, P. *Phys. Rev. Lett.* **1994**, *72*, 2109.
- (3) Leroux, N.; Mauzac, M.; Noirez, L.; Hardouin, F. *Liq. Cryst.* **1994**, *16*, 421.
- (4) Apfel, M. A.; Finkelmann, H.; Janini, G. M.; Laub, R. I.; Luhmann, B. H.; Price, A.; Robert, W. L.; Shaw, T. J.; Smith, C. A. *J. Am. Chem. Soc.* **1985**, *57*, 651.
- (5) Cagnon, M.; Durand, G. *Phys. Rev. Lett.* **1980**, *45*, 1418.
- (6) Adam, M.; Lairez, D. In *Physical Properties of Polymeric Gels*; Cohen-Addad, J. P., Ed.; John Wiley and Sons: New York, 1996.
- (7) This effect could explain why in ref 2, exponent x determined at 129 °C was found to be larger than 4. Another possible explanation is related to the fact that the measurements have been made by increasing the sample thickness and opening the cell for each thickness. This procedure may reduce the quality of the anchoring.
- (8) For instance, see: Stauffer, D. *J. Chem. Soc., Faraday Trans. 2* **1976**, *72*, 1354.
- (9) For instance, see: Stauffer, D. *Introduction to Percolation Theory*; Taylor and Francis: London, 1985.
- (10) This conclusion is also supported by experiments made in the nematic phase as a function of time, which show that G' remains constant even though the sample orients itself slightly during the experiment, owing to the grooves on the surface of the glass slides.
- (11) Colby, R. H.; Gillmor, J. R.; Galli, G.; Laus, M.; Ober, C. K.; Hall, E. *Liq. Cryst.* **1993**, *13*, 233.
- (12) Fridrikh, S. V.; Terentjev, E. M. *Phys. Rev. Lett.* **1997**, *79*, 4661.
- (13) Kannan, R. M.; Kornfield, J. A.; Schwenk, N.; Boeggel, C. *Macromolecules* **1993**, *26*, 2050.

MA981291N